ISSP

ACTIVITY REPORT OF SYNCHROTRON RADIATION LABORATORY

2023

Activity Report 2023
TABLE OF CONTENTS

1． Status of SARPES

Spin and angle-resolved photoemission spectroscopy (SARPES) stands as a powerful experimental technique that provides detailed information about the occupied electronic states in solids, including their energy, momentum, and spin. Recetnly, the growing interest in Rashba surface states and topological materials with spin-polarized electronic structures due to strong spin-orbit interactions has highlighted the importance of spin-resolved measurements. These spin-resolved experiments require high energy resolution and sufficient photoelectron yield rates to effectively detect small energy scales on the order of several meV. In response to these criteria, we successfully developed a high-energy resolution SARPES setup at the Laser and Synchrotron Research Center (LASOR) in the Institute for Solid State Physics (ISSP), using a vacuum-ultraviolet (6.994-eV) laser and spin detectors with the very-low-energy-electron-diffraction (VLEED) [1]. Since our initiative of developing the laser-SARPES in FY2014 and the commencement oft he facility for collaborative research in FY2015, our SARPES station has been instrumental in obtaining precise spin-resolved electronic structures near the Fermi level in solids.

Our laser-SARPES setup consists of an analysis chamber, a carousel sample-bank chamber connected to a load-lock chamber, and a molecular beam epitaxy (MBE) chamber, all connected via ultra high vacuum (UHV) gate valves. The hemispherical electron analyzer, a custom-made ScientaOmicron DA30-L, is designed to incorporate a VLEED-type spin detector. The available photon sources for electron excitation include the 6.994-eV laser, generated as the 6th harmonic of a high-power Nd:YVO4 quasi-continuous wave laser, and a helium discharge lamp (VG Scienta, VUV5000). In the MBE chamber, various instruments for surface evaluation and preparation, such as evaporators, low-energy electron diffraction, a sputter gun, and a quartz microbalance, can be installed, with samples heated by direct current heating or electron bombardment. The carousel chamber offers UHV storage for up to 16 samples. Spin-polarized states have been studied in both the bulk and surface of various topological materials, including magnetic and superconducting ones, atomic layers, and ferromagnetic compounds.

In FY2018, we began upgrading our laser-SAPRES system by integrating a pulsed laser to establish a pump-probe measurement setup. The newly installed pulsed 10.7-eV laser system [2,3], based on ytterbium fiber, achieves a 270-fs pulse duration, 1-MHz repetition rate, and high power through chirped pulse amplification, developed by the Kobayashi group at LASOR in ISSP[4]. This advanced system, as shown in Fig. 1, allows us to measure optically excited electron populations in unoccupied bands across the energy and momentum space and to track pump-induced ultrafast dynamics of both charge and spin. In addition to offering significant capabilities for the time-resolved measurements, the 10.7-eV laser system provides wider momentum information than lower photon energy sources such as 6.994-eV laser and offers better momentum resolution and polarization controls than the

helium discharge lamp. The polarization of the 10.7-eV probe laser, generated through third harmonic generation in Xe gas, can be selectively controlled using an MgF_2 half-wave plate, while the pump photon energy is selectable between 1.19-eV and 2.38-eV to accommodate a variety of band-gap materials. The original 6.994-eV light source remains available by adjusting mirrors and lenses in the vacuum beamline.

In FY2023, nine research proposals from external researchers were accepted and conducted using our SARPES setup, resulting in the publication of two research papers [4,5]. These proposed studies explored spin-polarized states across various platforms, including half-metallic ferromagnets, Dirac semimetals, topological insulators, two-dimensional materials, ferromagnetic oxides, and organic compounds. To support these advanced studies and further improve our experimental capabilities, we have also been focusing on upgrading the 10.7-eV laser system to enhance the stability of the pulsed light. This includes the development of laser evaluation systems, such as an autocorrelation measurement setup and Frequency-Resolved Optical Gating (FROG), as well as the integration of a new rod fiber amplifier into the system, which allows for higher output light.

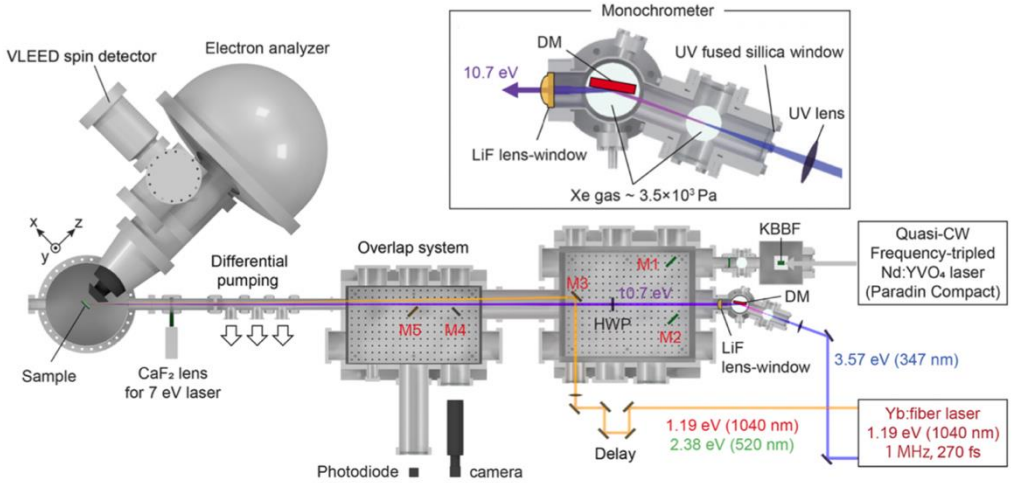

Fig. 1 Scaled layout of the 10.7-eV pulse laser beamline for tr-SARPES[4].

References:

[1] K. Yaji, A. Harasawa, K. Kuroda, S. Toyohisa, M. Nakayama, Y. Ishida, A. Fukushima, S. Watanabe, C.-T. Chen, F. Komori and S. Shin, Rev. Sci. Instrum. 87, 053111 (2016).

[2] Z. Zhao and Y. Kobayashi, Opt. Exp. 25, 13517 (2017).

[3] Z. Zhao, K. Kuroda, A. Harasawa, T. Kondo, S. Shin and Y. Kobayashi, Chin. Opt. Lett. 17, 051406 (2019).

[4] K. Kawaguchi, K. Kuroda, Z. Zhao, S. Tani, A. Harasawa, Y. Fukushima, H. Tanaka, R. Noguchi, T. Iimori, K. Yaji, M. Fujisawa, S. Shin, F. Komori, Y. Kobayashi, and T. Kondo, Rev. Sci. Instrum. 94, 083902 (2023)

[5] R. Moue, H. Yamazaki, T. Kitazawa, K. Yaji, H. Yaguchi, K. Kuroda, T. Kondo, A. Harasawa, T. Iwahashi, Y. Ouchi, S. Shin, and K. Kanai, Chem. Nano. Mat. 9, e202200538 (2023)

2. Activities at Sendai NanoTerasu

1. Transition to Sendai NanoTerasu and Facility Development

The management of the University of Tokyo high-brilliance, polarization-controlled 25-meter-long soft X-ray undulator beamline BL07LSU was transferred to the RIKEN SPring-8 Center in September 2022, marking the beginning of a new chapter for the organization. Following this transition, the Sendai office was established in November 2022 on the Aobayama campus of Tohoku University under the auspices of a new SRRO launched in April 2022, which includes six departments of the University of Tokyo. This strategic positioning facilitated the organization's involvement in the development of the new 3 GeV synchrotron facility NanoTerasu in Sendai, which began commissioning of its storage ring in early 2023.

At the end of fiscal year 2022, three critical endstations were relocated from SPring-8 to NanoTerasu: the ambient pressure X-ray photoemission spectroscopy (APXPS) station, the 3D-scanning photoelectron microscope (nanoESCA) station, and the high-resolution soft X-ray emission spectroscopy (HORNET) station.

2. Beamline Construction and Commissioning Activities

Throughout 2023, the Sendai office actively participated in establishing endstations at the soft X-ray beamlines BL07U and BL08U of NanoTerasu while collaborating with the Photon Science Innovation Center (PhoSIC) and the National Institutes for Quantum Science and Technology (QST) in the construction of these beamlines. The three endstations resumed commissioning activities during the summer of 2023 and were successfully realigned to their respective beamlines by the end of the fiscal year, with the nanoESCA and HORNET stations positioned at BL07U and the APXPS station at BL08U.

The infrastructure development proceeded smoothly throughout the year, with focusing mirrors and diffraction gratings installed upstream of both BL07U and BL08U beamlines. A significant milestone was achieved on December 7, 2023, when NanoTerasu successfully generated its first beam, marking the first introduction and observation of synchrotron radiation X-rays from insertion devices installed in the storage ring to the experimental hall.

3. Performance Evaluation and Technical Achievements

During the commissioning phase at the end of FY 2023, each endstation demonstrated preliminary operational capabilities. Optical adjustments for guiding synchrotron

radiation commenced in late February 2024, followed by actual delivery of synchrotron radiation to the endstations for equipment calibration, performance evaluation, and energy calibration. At BL08U, the APXPS system successfully achieved pressure ranges of 10-100 Torr for XPS measurements, maintaining its capability for operando observations of catalytic reactions at gas/solid interfaces. Upstream of the APXPS system a soft X-ray nano-focusing absorption spectroscopy apparatus was also installed. At BL07U, the 3DnanoESCA station obtained a spatial resolution of approximately 100-200 nm, enabling sub-microscopic chemical mapping and depth profiling capabilities. The HORNET station provided spectra with energy resolution around 500 meV at 500 eV, supporting high-resolution soft X-ray emission spectroscopy measurements.

4. Future Prospects and Operational Preparation

On March 25, 2024, the Sendai office completed its relocation to the SRIS (International Center for Synchrotron Radiation Innovation Smart) building of Tohoku University from the Agricultural Research Building to the SRIS building within the Aobayama campus of Tohoku University, positioning itself as one of the facilities closest to NanoTerasu. The SOR member at the Sendai office continued working toward the commencement of operations in the beginning of April 2024. Young staff members are actively engaged in developing related technologies to support these advanced capabilities.

While current achievements at NanoTerasu remain considerably below the standards established at SPring-8, significant improvements are anticipated as the beamlines undergo final alignment procedures following the official commencement of operations in April 2024. The foundation established during this transitional year positions the facility to recover and ultimately exceed the performance criteria previously achieved, enabling advanced soft X-ray spectroscopy research and operando experimental capabilities for the broader scientific community.

3 . Seminar

SOR Seminar

Date: July 24, 2023

Title: Active Dopant Sites in Si Hyperdoped with Te Investigated by Photoemission

Speaker: Dr. Moritz Hoesch (Deutsches Elektronen-Synchrotron DESY, Photon Science, Hamburg)

LASOR Seminar

Date: July 24, 2023

Title: Research on cathodes of lithium-ion batteries by synchrotron soft X-ray spectromicroscopy

Speaker: Dr. Zhang Wenxiong (ISSP, The University of Tokyo)

LASOR Seminar

Date: November 20, 2023

Title: Ultracompact mirror device for forming 20-nm achromatic soft-X-ray focus toward multimodal and multicolor nanoanalyses

Speaker: Dr. Takenori Shimamura (ISSP, The University of Tokyo)

OBSERVATION OF ELECTRONIC STRUCTURE OF SELF-ASSEMBLED ORGANIC KAGOME LATTICE USING COORDINATION BONDS

Kaname Kanai
Department of Physics and Astronomy, Faculty of Science and Technology, Tokyo University of Science

Kagome lattice has a structure that is a combination of a triangular lattice and a honeycomb lattice, which is theoretically predicted to realise specific electronic states such as Dirac bands and flat bands. In particular, flat band is highly localized state resulting from the destructive interference of the wavefunction of the conduction electrons, and is thought to be the origin of specific physical properties such as superconductivity and ferromagnetism through strong correlation effects. Although several reports have claimed to have experimentally observed flat bands in Kagome lattices, most of them actually show some dispersion width and are not completely flat bands. The reason for this is that a Kagome lattice in a three-dimensional crystal is hardly a perfect two-dimensional Dirac system [1], and therefore not an ideal Kagome lattice. To solve this problem, it has been reported that organic molecules with three-fold symmetry were adsorbed on a noble metal surface to form a Kagome lattice in a two-dimensional system in a self-assembling manner using intermolecular hydrogen bonds, and flat bands were observed by angle-resolved photoemission spectroscopy (ARPES) [2]. However, even in this system, the intermolecular hydrogen bonds distort the molecular shape and the resulting Kagome lattice is not an ideal two-dimensional system.

The aim of this study is to form an ideal Kagome lattice by fabricating a self-assembled film with THPB (1,3,5-tris(4-hydroxyphenyl)benzene) and to directly observe its electronic structure by ARPES. As shown in Figure 1, THPB is an organic molecule with a three-fold symmetrical structure and a hydroxy group at the molecular terminals. From previous study [2], THPB is known to form a Kagome lattice-like self-assembled monolayer on Au(111), but because of the hydrogen bonding network, the π-orbital is almost localised to each molecule and cannot be regarded as forming a Kagome lattice. Therefore, Cu(111) was employed as a substrate in this study. In general, when a copper substrate is used, copper atoms easily diffuse into the organic thin film formed on it. Taking advantage of the unique properties of this copper substrate, the present study tries to prepare an ideal Kagome lattice by incorporating copper atoms in the THPB thin film. First, a monolayer of THPB is formed on Cu(111) by vacuum evaporation, followed by annealing, which leads to dehydrogenation of the three hydroxy groups of THPB. The copper atoms diffusing from the substrate into the THPB film then coordinate into the voids of the three THPB molecules, forming a Kagome lattice. In general, such two-dimensional organic structures bridged by metal atoms are called metal-organic framework (MOF).

In the present study, energy band calculations based on density functional theory (DFT) were first performed to ascertain whether, in fact, the THPB-MOF could be an ideal Kagome lattice. Figure 1(a) shows the result of the calculation. As depicted in the figure, the structure with three copper atoms ligated between three THPB molecules is the most stable. The calculated energy band structure does indeed show the Dirac and flat bands characteristic of the Kagome lattice. The two Dirac cones contact at point K and a Dirac point exists. On the other hand, an ideal flat band is seen at the top of the upper Dirac cone, where the energy is completely independent of the wavenumber. Our calculations have also confirmed that such an ideal Kagome lattice band structure cannot be achieved in the THPB Kagome lattice generated through the intermolecular hydrogen bonds.

The LEED results of the THPB monolayer on Cu(111) are then shown in Fig. 1(b). The right semicircle shows the measured LEED pattern and the left semicircle shows the LEED pattern obtained by simulation.

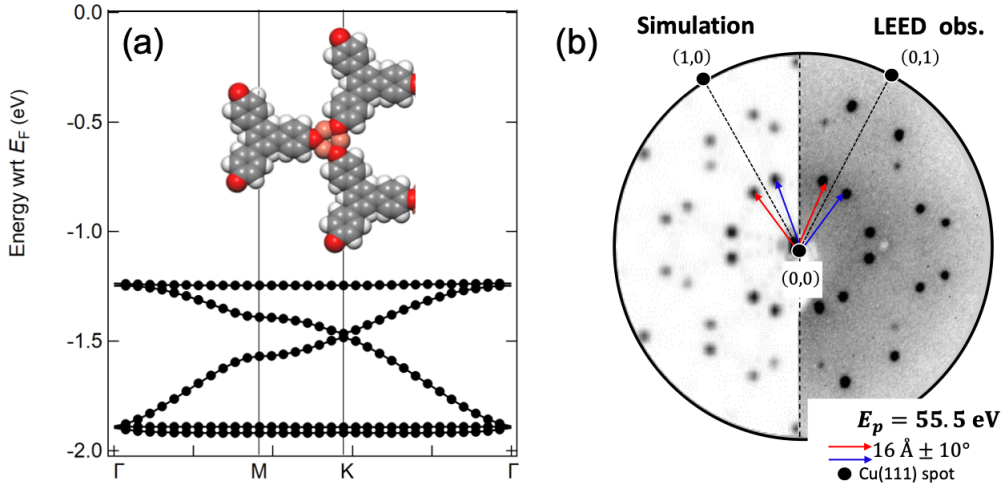

Figure 1. a) Energy band structure of THPB-MOF obtained by the DFT calculation. The grey, white and red balls in the molecular structure in the figure represent carbon, hydrogen and oxygen, respectively. The pink ball represents copper. b) The LEED results of the THPB monolayer on Cu(111). The right semicircle shows the measured LEED pattern (LEED obs.) and the left semicircle shows the LEED pattern obtained by simulation (Simulation). The primary energy for the LEED measurements was set at 55.5 eV.

The observed and simulated LEED results are in good agreement. The structure of the THPB monolayer obtained from this analysis is shown in Figure 2.

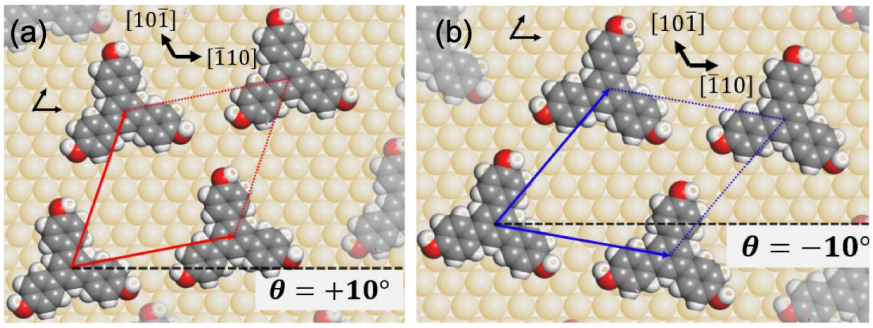

Figure 2. The structures of THPB monolayer on Cu(111) obtained by the analysis of the LEED results. (a) The domain tilted 10° from the [-110] direction of Cu(111) and (b) -10°.

The THPB monolayer was found to have two domains inclined 10° or -10° from the [-110] direction of Cu(111). These domains have a Kagome lattice structure. Therefore, a Kagome lattice has been successfully grown on Cu(111) by THPB. The next stage of this research will be to confirm that the copper atoms are actually incorporated into the monolayer as a THPB-MOF and to directly observe its electronic structure by ARPES.

REFERENCES

[1] Z, Liu *et al*., *Nat. Commn.*, **11**, 4002 (2020).
[2] M. Pan *et al*., *Phys. Rev. Lett.*, **130**, 036203 (2023).

SARPES STUDY OF CVD-GRAPHENE ON FERROMAGNETIC NI (111) SUBSTRATE

Thang Dinh Phan[1], Shunsuke Tsuda[1], Yuto Fukushima[2], Kaishu Kawaguchi[2], Ryo Mori[2], Takeshi Kondo[2], Koichiro Yaji*[1,3]

[1] *Center for Basic Research on Materials, National Institute for Materials Science (NIMS), Tsukuba 305-0003, Japan*

[2] *The Institute for Solid State Physics, The University of Tokyo, Kashiwa, 77-0882, Japan*

[3] *Unprecedented-scale Data Analytics Center, Tohoku University, Sendai 980-8578, Japan.*

**e-mail: YAJI.Koichiro@nims.go.jp*

Recently, graphene has emerged as an extraordinary modern material for realizing novel spintronic devices due to the long spin lifetime and long spin relaxation length reflecting the weak spin-orbit interaction, hyperfine interaction, and the specific π band structure. Therefore, studying the transport of spin-polarized electrons in graphene has attracted significant attention from experimentalists and theorists as a fascinating area of research and development. In previous studies, spin polarization in single-layer graphene is induced by some phenomena such as spin-orbit interaction [1,2], strong hybridization between graphene and substrate [3-5], and proximity magnetization [6].

In this study, we have investigated the spin polarization of graphene on Ni (111) film by angle-resolved photoemission spectroscopy (ARPES) and spin- and angle-resolved photoemission spectroscopy (SARPES) at the Institute for Solid State Physics (ISSP), the University of Tokyo [7]. The Ni(111) film is prepared on a sapphire (SAP) substrate. The graphene is fabricated on the Ni(111) film using the chemical vapor deposition (CVD) technique. The *x*-(*y*-)axis coincides with the $\overline{\boldsymbol{\Gamma K}}$ ($\overline{\boldsymbol{\Gamma M}}$) direction of the first Brillouin zone of graphene [Fig. 1(a)]. Before the SARPES measurements, the sample was magnetized parallel to the *y*-axis, and thus, we detected the *y*-spin component in SARPES.

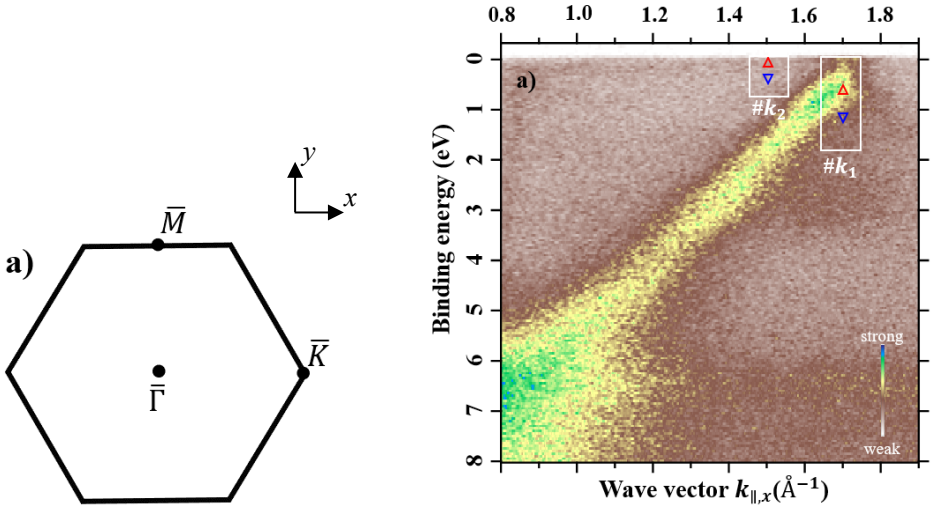

Fig. 1 (a) The Brillouin zone of graphene. (b) The ARPES mapping of the π band of CVD-grown graphene on Ni(111). The red and blue symbols represent the peak positions of the spin-resolved photoemission spectra.

Figure 1(b) shows the ARPES intensity mapping of the π band of CVD-grown graphene on Ni(111). The Dirac point nearly reaches the Fermi level in contrast to that reported in the previous study [3-5]. The SARPES measurements were performed at selected *k*-points ($\#k_1$ and $\#k_2$). The red and blue triangles give the peak positions of the spin-resolved photoemission spectra. At $\#k_1$, the spin polarization is observed near the Dirac point, where the +*y* (-*y*) spin state is found at a binding energy of 0.8 eV and 1.1 eV. We also observe the spin

polarization at a binding energy of 0.18 eV and 0.24 eV at $\#k_2$.

The proximity effect with the Ni substrate can cause the spin polarization observed in the π band of graphene. On the other hand, the spin polarization at $\#k_2$ is attributed to the exchange splitting of the Ni(111) electronic states.

References

[1] N. Tombros, C. Jozsa, M. Popinciuc, H. T. Jonkman, and B. J. Van Wees, Nature, vol. 448, no. 7153, pp. 571–574 (2007).

[2] W. Han et al., Phys Rev Lett, vol. 105, no. 16 (2010).

[3] D. Marchenko, A. Varykhalov, J. Sánchez-Barriga, O. Rader, C. Carbone, and G. Bihlmayer, Phys Rev B, vol. 91, no. 23 (2015).

[4] A. Varykhalov et al., Phys Rev X, vol. 2, no. 4 (2012).

[5] D. Usachov et al., Nano Letters 2015, 15, 4, 2396-2401.

[6] Q. F. Sun, Z. T. Jiang, Y. Yu, and X. C. Xie, Phys Rev B, vol. 84, 214501 (2011).

[7] K. Yaji et al., Rev. Sci. Instrum. 87, 053111 (2016).

TIME-RESOLVED SPIN-RESOLVED HIGH-RESOLUTION PHOTOEMISSION SPECTROSCOPY OF HALF-METALLIC FERROMAGNETS

Hirokazu FUJIWARA,[1,2] Tomoki HIGASHIKAWA,[3] Lingling XIE,[4] Daisuke KAN,[4] Yuichi SHIMAKAWA,[4] Kaishu KAWAGUCHI,[5] Ryo MORI,[5] Ayumi HARASAWA,[5] Takeshi KONDO,[5] Takayoshi YOKOYA[3,6]

[1]*Material Innovation Research Center (MIRC), The University of Tokyo*
[2]*Graduate School of Frontier Science, The University of Tokyo*
[3]*Graduate School of Environment, Life, Natural Science and Technology, Okayama University*
[4]*Institute for Chemical Research, Kyoto University*
[5]*Institute for Solid State Physics, The University of Tokyo*
[6]*Research Institute for Interdisciplinary Science, Okayama University*

Half-metallic ferromagnets have a unique spin dependent electronic structure near the Fermi level (E_F), where only one of the spin states crosses E_F while the other has an energy gap across E_F.[1] The unique electronic structure gives rise to many-body effects different from other systems. Theoretically, the electronic states induced by many-body effects in half metals has been proposed as non quasiparticle (NQP) states.[2] The experimental verification for NQP states was made recently for a type-I_A half metallic ferromagnet CrO_2 by using high-resolution (HR) spin-resolved photoemission spectroscopy (SRPES).[3] In the present study, we have performed HRSRPES of a candidate for a half-metallic ferromagnet $NiCo_2O_4$ (NCO) to investigate the evolution of NQP states with increasing temperature, as a preliminary experiment for time-resolved measurements. From first-principles calculation, NCO is predicted to be a type-I_B half-metal in which only the minority spin bands crosses E_F, and NQP states are expected to appear below E_F.[4,5]

Epitaxial films of NCO were grown on the (001) surface of $MgAl_2O_4$ substrates using a pulsed laser deposition method.[6] The Curie temperature is approximately 400 K.[6] Laser-based HRSRPES experiments were performed at the Institute for Solid State Physics, The University of Tokyo.[7] The p-polarized light with $h\nu$ = 6.994 eV was used to excite the photoelectrons. Photoelectrons were analyzed with a combination of a ScientaOmicron DA30L analyzer and a very low energy electron diffraction (VLEED) type spin detector. During the measurement, the instrumental energy resolution was set to 30 meV, and the base pressure was kept below 1×10^{-8} Pa. Calibration of E_F for the samples was achieved using a gold reference. The data were acquired at T = 20 K, 40 K, 60 K, 80 K, 100 K, 130 K, 160 K, 180 K, 200 K, 250 K, and 300 K. The samples were magnetized along the magnetic easy axis corresponding to the out-of-plane axis of the film ([001] direction) by using MPMS system.

Figure 1 shows the temperature dependent HRSRPES data. At 20 K, the spectrum of the minority spin states shows a clear Fermi edge, while that of the majority spin states goes towards 0 as the energy approaches E_F. The decrease in the intensity of the majority spin states corresponds to a sharp increase in spin polarization (blue arrow). The absence of a clear Fermi edge in the majority spin spectrum experimentally suggests that NCO is a type-I_B half-metallic ferromagnet.

With increasing temperature, no significant change was observed up to 100 K, but from around 130 K, the slope of the sharp increase of the spin polarization towards E_F become smaller. This indicates that the majority spin states near E_F are broadened significantly more than the temperature dependence of the Fermi-Dirac distribution function. Such broadening, which occurs as the majority spin states fill the gap, is consistent with the temperature-dependent behavior of NQP states.[1]

As the temperature is further increased, a decrease in spin polarization is also observed in the low-energy region below –0.1 eV from 200 K. The temperature dependence of the spin

polarization at the low energy region is in good agreement with the temperature dependence of the macroscopic magnetization. This indicates that the depolarization can be attributed to spin wave excitations,[3] and that the bulk electronic states of NCO are dominantly observed in this measurement.

In summary, we investigated NCO which is a candidate for a type-I_B half-metallic ferromagnet. At 20 K, we observed a sharp increase in spin polarization toward E_F and a corresponding sharp decrease in the density of majority spin states. This is characteristic of type-I_B half-metallic ferromagnets. Furthermore, we observed the broadening of the majority spin states above 130 K. This behavior is consistent with that of NQP. This study provides experimental insight into the half-metallicity of NCOs and may be the first demonstration of NQP in type-IB half-metals.

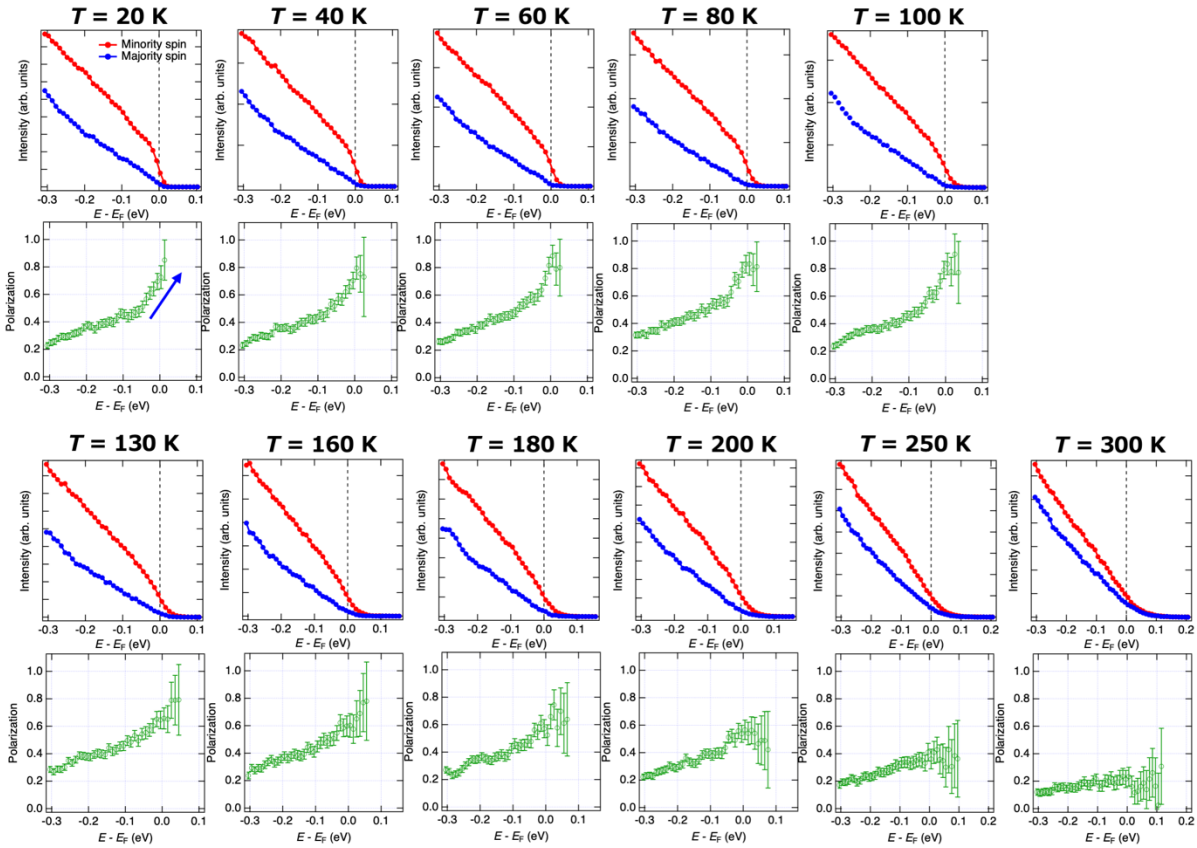

Fig. 1. Temperature dependent HRSRPES spectra and spin polarizations of NCO.

ACKNOWLEDGEMENT

This work was partially supported by JSPS KAKENHI Grant Number (23H01125) from MEXT.

REFERENCES

[1] M.I. Katsnelson *et al.*, Rev. Mod. Phys. **80**, 315 (2008).
[2] V.Y. Irkhin and M.I. Katsnelson, Usp. Fiz. Nauk **164**, 705 (1994).
[3] H. Fujiwara *et al.*, Phys. Rev. Lett. **121**, 257201 (2018).
[4] D. Dileep *et al.*, J. Phys. D: Appl. Phys. **47**, 405001 (2014).
[5] V. Yu. Irkhin and M. I. Katsnelson, Eur. Phys. J. B **43**, 479 (2005).
[6] Y. Shen *et al.*, Phys. Rev. B **101**, 094412 (2020).
[7] K. Yaji e*t al.*, Rev. Sci. Instrum. **87**, 053111 (2016).

STUDY OF ATTOSECOND PHOTOEMISSION DYNAMICS THROUGH PHOTOELECTRON SPIN INTERFERENCE

Kenta Kuroda[1,2,3,] Towa Kosa[1], Takuma Iwata[1,2], Kaishu Kawaguchi[4], Yuto Fukushima[4], Ryo Mori[4], Takeshi Kondo[4], Shik Shin[4], Koichiro Yaji[5] and Fumio Komori[6]

[1]*Graduate School of Advanced Science and Engineering, Hiroshima University, Japan*

[2]*WPI-SKCM[2], Hiroshima University, Japan*

[3]*Research Institute for Semiconductor Engineering, Hiroshima University, Japan*

[4]*Institute for Solid State Physics, The University of Tokyo, Japan*

[5]*Research Center for Advanced Measurement and Characterization, NIMS, Japan*

[6]*Institute of Industrial Science, The University of Tokyo, Japan*

The realization of spin-polarized electrons and their manipulation are the main goal in the field of spintronics. A promising way is by utilizing materials with strong spin-orbit coupling (SOC). The representative examples are Rashba systems and topological insulators, at surfaces of which spin-polarized electrons emerge due to antisymmetric SOC under the lack of inversion symmetry. As a consequence of SOC, the different spin and orbitals are entangled, which can be directly probed by spin- and angle-resolved photoemission spectroscopy (SARPES). Since light polarization can select the orbital part of the wave functions, this entanglement allows us to optically control the electron spin, leading to optospintronic functions.

By previous SARPES studies on the surface state of Bi_2Se_3 [1, 2] and Bi(111) [3], it was demonstrated that *p*- or *s*-polarized light can selectively excite spin-polarized photoelectrons with either spin-up or spin-down from the wave function. By using a tilted linear polarization with both *p*- and *s*-polarization components, both spin states are excited simultaneously and interfere in photoelectron states [Fig. 1], which can be seen as a rotation of the spin orientation from the initial helical-spin state [1-3].

While the above experiments greatly facilitate an optical spin manipulation by a proper light polarization, the biggest advantage of looking at this spin interference phenomena is that one can determine a relative phase difference between the two processes (T_p and T_s), excited either by *p*- or by *s*-polarized light [Fig. 1, 1-3]. Yet, the physical origin of the phase in the spin interference and its interpretation remain unsolved questions.

Fanciulli and Dil *et al* suggested that the phase difference reflects time scale of photoemission dynamics [4]. According to their claim, the phase information, determined by photoemission spectroscopy, can be converted to a delay time of the photoemission processes as follows:

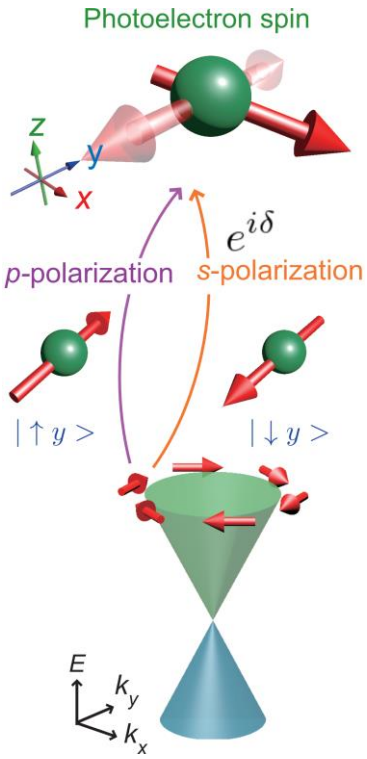

Fig. 1: Superposition of spin-up and spin-down in a photoelectron fina state excited from the Dirac surface state of Bi_2Se_3 [1, 2].

$$\tau = \hbar|\frac{\partial\phi}{\partial E_k}|$$

where τ, ϕ, and E_k are a delay time, a phase difference, and a kinetic energy of photoelectrons. This formula is obtained by a simplest model, called Eisenbud-Wigner-Smith (EWS) model [4], in which the free electrons scattered by short-range potential are considered and the phase between the incoming and outcoming electrons is shifted. The EWS time is, thus, considered as a sticking time in the interaction potential.

To experimentally determine the kinetic energy dependence of the phase, we used SARPES with 7-eV laser at ISSP [5] and with 6-eV laser at HiSOR [6]. Figures 2(a) and (b) summarize the spin polarization vector of the photoelectrons emitted from the surface state of Bi_2Se_3 at two different kinetic energies obtained by laser-SARPES with 7-eV laser. Apparently, the spin polarization vector sensitively relies on the kinetic energy. Figures 2(c) and (d) maps the spin information into Bloch sphere, displaying how the phase deviates in the photoelectron final states. Surprisingly, our additional observations using laser-SARPES with 6-eV laser demonstrate that the observed spin polarization is insensitive to the kintic energy, which shows sharp contrast to the results for 7-eV laser-SARPES. This large contradiction between the two independent measurements implies that the spin interference effect is dominated by the final state characters that can be selected by photon energies in SARPES measurements.

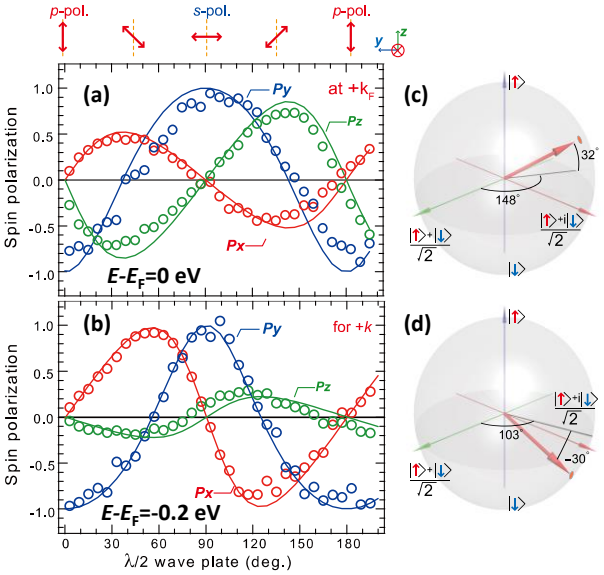

Fig. 2: SARPES results with 7-eV laser at ISSP. (a, b) Linear-polarization evolutions of the three-dimensional spin polarization, $P_{x,y,z}$, of the photoelectrons emitted from the surface state of Bi_2Se_3. (c, d) The spin-polarization mapped into Bloch spehere considereing a superposition of spin-up and spin-down eigenstates.

REFERENCES

[1] Kenta Kuroda, Koichiro Yaji *et al.*, Phys. Rev. B **94**, 165162.
[2] Kenta Kuroda, Koichiro Yaji *et al.*, Phys. Rev. B **105**, L121106 (2022).
[3] Koichiro Yaji and Kenta Kuroda *et al.*, , Nat. Commun. **8**, 14588 (2017).
[4] Mauro Fanciulli *et al.*, Phys. Rev. Lett. **118**, 067402 (2017).
[5] Koichiro Yaji *et al.*, Rev. Sci. Instrum. **87**, 053111 (2016).
[6] Takuma Iwata *et al.*, Sci. Rep. **14**, 127 (2024).

INVESTIGATION OF SURFACE STATES OF FERROMAGNETIC TOPOLOGICAL SEMIMETAL CoS_2

Yuting Qian, Younsik Kim, Changyoung Kim, and Bohm-Jung Yang
Department of Physics and Astronomy, Seoul National University

Floating surface states (FSSs) are a new type of surface states, which spread over the entire Brillouin zone (BZ) [1–3]. This property is different from conventional based surface states (BSS) whose location in the momentum space is bounded by the symmetry or the nodal structure of bulk bands (see Figure 1). Although the presence or absence of FSS is termination dependent due to its atomic nature, it can be potentially more important to design surface-sensitive functionality due to its extended character. In particular, in topological materials that are intrinsically three-dimensional (3D) and not layered, the surface functionality can strongly depend on the surface termination and its orientation because of the termination dependent FSSs of topological or non-topological origin. A spin-orbit-coupled ferromagnetic pyrite CoS_2 has a great potential to exhibit FSSs since CoS_2 is an intrinsically 3D material with covalent bonds of nearly equal strength in all 3D directions. Based on this motivation, we investigated the surface electronic states of CoS_2 by laser-based angle-resolved photoemission spectroscopy (ARPES).

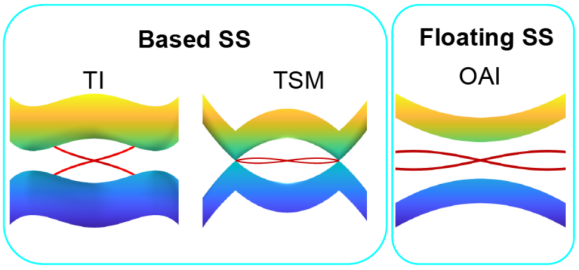

Figure 1. The two types of surface states (SSs) are depicted schematically: based SS (BSS) and floating SS (FSS).

Single crystals of CoS_2 were grown using a chemical vapor transport method with Br agent. The grown samples exhibit a ferromagnetic transition at 120 K. ARPES data were acquired by laser-based spin-resolved ARPES system at the Institute for Solid State Physics, University of Tokyo. All the ARPES measurements were conducted using 6.994 eV light. The samples were cleaved along the (001) direction at 15 K and subsequently magnetized along the (010) direction by bringing a magnet close to the sample. We note that the magnetization was conducted in the Carousel chamber, as we cannot bring the magnet into the main chamber.

Figure 2(a) shows the ARPES result near the Γ point. We could observe a hole-like band. The observed band structure is consistent with the slab calculation result with 1S termination, shown in Figure 2(b). Thus, the observed band structure can be attributed to the FSS originated from 1S termination. Based on the measured band structure, we subsequently conducted spin-ARPES measurements after magnetizing the sample. Despite multiple attempts, we could not observe any spin polarization of the surface state as shown in Figure 2(c). However, the slab calculation indeed predicts spin polarization of the corresponding band. We speculate that the discrepancy stems from incomplete magnetization and the soft nature of the ferromagnetism of CoS_2.

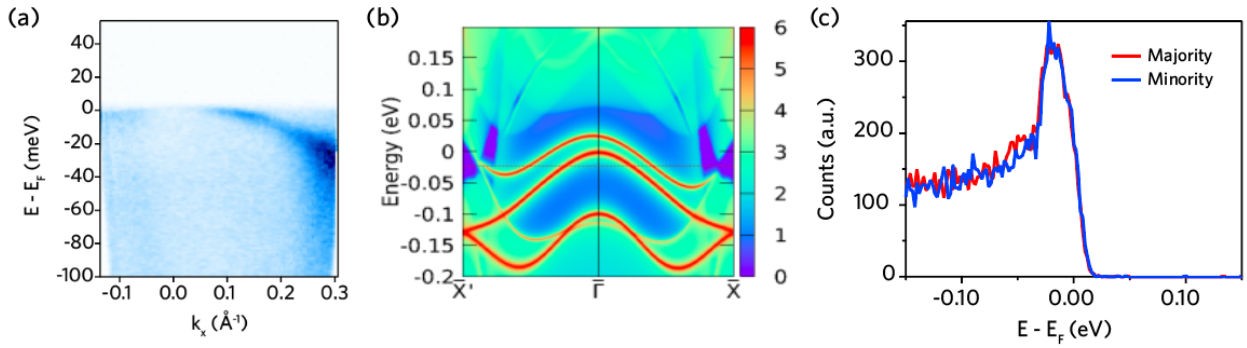

Figure 2. (a) Laser-based ARPES result on CoS_2 near the Γ point. (b) Slab calculation result on 1S termination of CoS_2 (c) Spin-resolved photoemission result at the Fermi momentum.

In summary, we successfully measured the FSS of the CoS_2 using laser-based ARPES. However, we could not observe spin polarization of the FSS, which is predicted by the slab calculations.

REFRENCES

[1] Motoaki Hirayama, Satoru Matsuishi, Hideo Hosono, and Shuichi Murakami, Phys. Rev. X 8, 031067 (2018).

[2] Simin Nie, Yuting Qian, Jiacheng Gao, Zhong Fang, Hongming Weng, and Zhijun Wang, Phys. Rev. B 103, 205133 (2021).

[3] Jiacheng Gao, Yuting Qian, Huaxian Jia, Zhaopeng Guo, Zhong Fang, Miao Liu, Hongming Weng, and Zhijun Wang, Science Bulletin 67, 598–608 (2022).

SARPES on TiSe2 and CuTe 3-10 JULY 2023

Fei Guo, Hugo Dil
Institute of Physics, École Polytechnique Fédérale de Lausanne, CH-1015 Lausanne, Switzerland
Mauro Fanciulli
Laboratoire de Physique des Matériaux et Surfaces, CY Cergy Paris Université, 95031 Cergy-Pontoise, France

Overview

The objective of our experiment was to study the spin polarization of photoelectrons from the charge-density-wave materials CuTe and $TiSe_2$ at low photon energy with high resolution. With the spin polarization as a function of binding energy, we would then be able to estimate the Eisenbud-Wigner-Smith (EWS) time delay of photoemission as explained in ref.[1]. While this time delay has been estimated for both materials at high photon energies, it would be useful to compare them to the one obtained from low photon energy results in order to investigate how different photoemission final states affect the EWS time scale. However, for both CuTe and $TiSe_2$ the experiment yielded unexpected yet valuable results.

Quality of measurement/data

Thanks to the well-maintained spin-ARPES end station and high-efficiency VLEED spin detectors, spin-resolved bandmaps could be taken with high statistics in all 3 spatial spin directions. The efficient end station, stable light source and excellent support from the lab members allowed us to measure more, and higher-statistics spin-resolved data than expected, and many of them are of significant interest, and are currently being analysed in-depth.

Status and progress of evaluation

The high-quality spin-resolved data allows us to do a quantitative study in order to estimate the EWS time scale for CuTe, and the comparison between the time scales estimated from low- and high-photon energy measurements gives valuable hints about photoemission final state effects. The unexpected spin texture of $TiSe_2$ seen with low photon energy also points to different selection rules dictated by the final state, and it shows agreement with preliminary one-step photoemission calculations. We are currently wrapping up the analysis and will write manuscripts to be submitted for publication soon.

Results

For CuTe, our objective was to measure spin polarization on the bands around the **Γ** point. However, at photon energy $h\nu$=6.994eV, we only observe a band that was not visible at high photon energies, the corresponding bandmap is shown in Fig.1(a), in comparison to bandmap at high photon energy in Fig.1(b). This observed band is spin polarized mostly in the in-plane y-direction, as shown in Fig.1(c). In order to estimate the EWS time delay associated with the observed band, for each kinetic energy the peak spin polarization in y is recorded as a data point of spin polarization versus binding energy. From this, the EWS time delay is estimated as $|\tau_{EWS}| \geq \hbar \left|\frac{dP}{dE_K}\right| \approx 0.984 \times 10^{-16} s \approx 98.4$ as. This is much shorter compared to the EWS time scale we measured at the higher photon energy of $h\nu$=26eV, at which we obtained

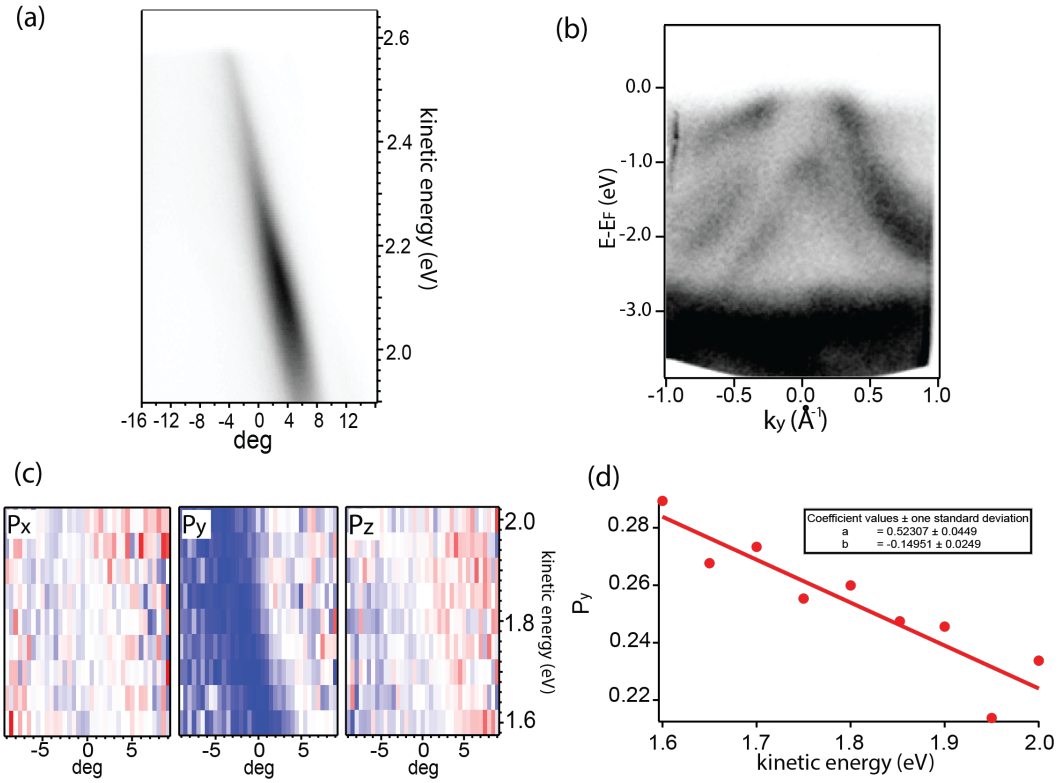

Figure 1: (a) Bandmap taken for CuTe around Brillouin zone center with $h\nu$=6.994eV, (b) bandmap taken for CuTe around Brillouin zone center with $h\nu$=40.35eV, (c) spin-resolved bandmap of the band shown in (a) with spin components in all 3 directions, (d) maximum y-polarization of spin extracted from (c) as a function of kinetic energy.

$|\tau_{EWS}| \geq \hbar \left|\frac{dP}{dE_K}\right| \approx 210$ as. Furthermore, at both low and high photon energies, we observe a so-called double polarization feature, i.e. a spin polarization of opposite sign at different sides of the intensity maximum. This is shown in Fig.2(a) and (b) for $h\nu$=6.994eV and $h\nu$ =26eV respectively. Along with this same effect observed for many systems including Cu(111) and BSCCO-2212, we can confirm that this is a common feature of spin polarization in spin degenerate states.

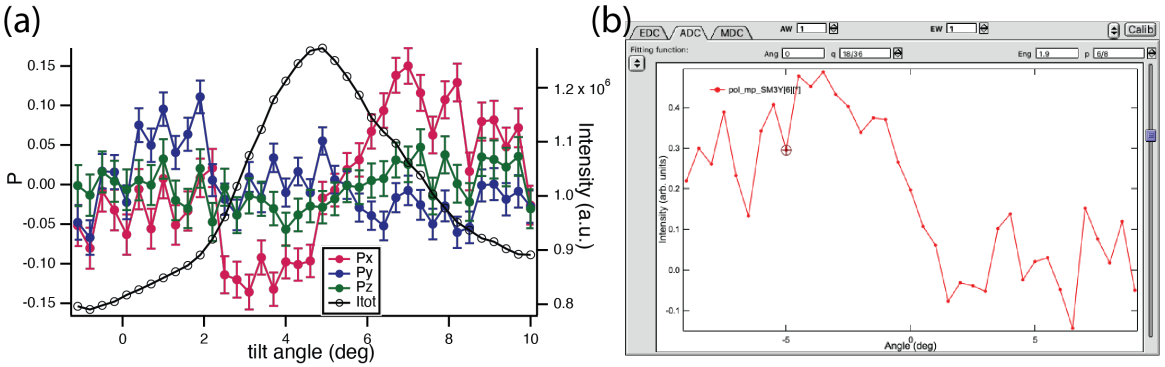

Figure 2: (a) Spin polarization of CuTe in all 3 directions taken at photon energy $h\nu$=26eV and binding energy 0.6eV, (b) spin polarization of CuTe in the y-direction taken at photon energy $h\nu$=6.994eV and binding energy 0.6eV, image sliced from Fig.1(c).

For $TiSe_2$, our objective was also to measure the spin polarization around **Γ**. However, the observed spin texture at low photon energy is completely unexpected. Specifically, the spin polarization on both sides of **Γ** is symmetric, and there is a strong out-of-plane spin polarization at **Γ**, as shown in Fig.3(a), in which the polarization varies from around -25% to +40%, as shown in Fig.3(d). With a different measurement orientation, as shown Fig.3(b), or a different light polarization, as shown in Fig.3(c), this out-of-plane spin polarization is always present. We have also measured the spin polarization at **Γ** as a function of light polarization as shown in Fig.3(e), to further characterise this effect.

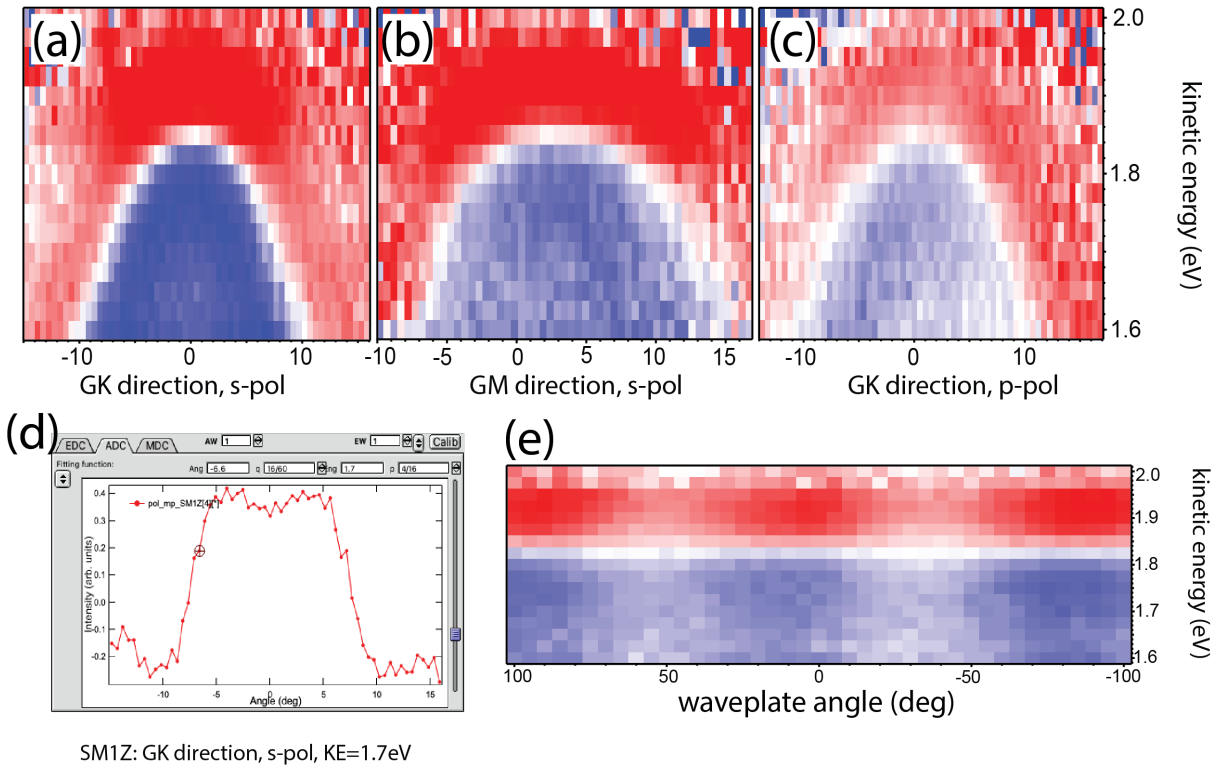

Figure 3: (a-c) Spin-polarized bandmap of $TiSe_2$ taken in **Γ**-K and **Γ**-M orientations, with s- and p-polarized light, (d) spin polarization of $TiSe_2$ in the z-direction, taken in the **Γ**-K orientation and with s-polarized light, at binding energy 0.8eV, (e) spin polarization EDC at the **Γ** point as a function of wave plate angle.

REFERENCES

[1] M. Fanciulli, H. Volfová, S. Muff, J. Braun, H. Ebert, J. Minár, U. Heinzmann, and J. H. Dil, Physical Review Letters 118, 067402 (2017)

5. Staff

Director: HARADA Yoshihisa, Professor
MATSUDA Iwao, Professor
KIMURA Takashi, Associate Professor
KONDO Takeshi, Associate Professor
HORIO Masafumi, Research Associate
KIUCHI Hisao, Research Associate
TAKEO Yoko, Research Associate
MORI Ryo, Research Associate
SHIMAMURA Takenori, Project Research Associate (2023.10~)
HARASAWA Ayumi, Leading Senior Technical Specialist
KUDO Hirofumi, Senior Technical Specialist

Project Academic Specialist:
FUKUSHIMA Akiko (~2024.3)
SHIBUYA Takashi
KOSEGAWA Yuka

Secretary:
AIHARA Yumiko
YOSHIZAWA Motoko
SHIBATA Ayako
SASAKI Sonomi (2023.7~)
NORO Mariko (2024.1~)

Project Researcher:
OHDAIRA Takeshi
ZHANG Wenxiong
KITAKATA Emi
Al Samarai Mustafa
LIU Daobin (~2024.2)
NIIBE Masahito
TANG Jingmin
KAWAHARA Kotaro (2023.12~2024.3)

Graduate Student:
UGALINO Ralph John
SATO Yusuke
TSUJIKAWA Yuki
YANG Tianqi
SUMI Toshihide
WADA Tetsuya
TOMIYORI Yusuke
LI Hao
ZHANG Xiaoni
ZHAO Haochong
SAKURAI Kai
YIN Heming
HUA Yangyang
YOSHINAGA Kyota
YAMAGUCHI Kazuki
MIYAMOTO Masashige
GUAN Yanze
ZHANG Menghan
SU Xingyu
ZENG Yanquan
SAKURAI haruto
NAKATA Yu

Harima Paper 2023

No	Title	Authors	Journal	Vol.	No.	Page	年
1	Hydrogen-bonded Structure of Hydrated Water in Polyvinyl Pyrrolidone Aqueous Solution Investigated by X-ray Absorption and Emission Spectroscopy	Koichi Ozaki , Masaru Nakada , Masahiro Kunisu , Jumpei Yahiro , Kosuke Yamazoe , Yitao Cui , Jun Miyawaki , Yoshihisa Harada	Journal of Molecular Liquids	403		124822	2024
2	軟X線発光分光で見る水の水素結合とオペランド分光への展開	原田慈久	表面と真空	67	5	224-228	2024
3	The role of carboxylate ligand orbitals in the breathing dynamics of a metal-organic framework by resonant X-ray emission spectroscopy	Ralph Ugalino , Kosuke Yamazoe , Jun Miyawaki , Hisao Kiuchi , Naoya Kurahashi , Yuka Kosegawa , Yoshihisa Harada	Journal of Synchrotron Radiation	31		217-221	2024
4	Angle-resolved X-ray emission spectroscopy facility realized by an innovative spectrometer rotation mechanism at SPring-8 BL07LSU	Jun Miyawaki, Yuka Kosegawa and Yoshihisa Harada	Journal of Synchrotron Radiation	31	2	208-216	2024
5	Quasi-Periodic Growth of One-Dimensional Copper Boride on Cu(110)	Yuki Tsujikawa, Xiaoni Zhang, Kazuki Yamaguchi, Masahiro Haze, Takeru Nakashima, Arpita Varadwaj, Yusuke Sato, Masafumi Horio, Yukio Hasegawa, Fumio Komori, Masaki Oshikawa, Masato Kotsugi, Yasunobu Ando, Takahiro Kondo, Iwao Matsuda	Nano Letters	24		1160-1167	2024
6	Revealing the Unusual Mechanism of Mixed Cationic and Anionic Redox in Oxyfluorosulfide Cathode for All-Solid-State Fluoride-Ion Batteries	Zulai Cao, Kentaro Yamamoto, Toshiyuki Matsunaga, Toshiki Watanabe, Mukesh Kumar, Neha Thakur, Ryogo Ohashi, Shintaro Tachibana, Hidenori Miki, Kazuto Ide, Hideki Iba, Hisao Kiuchi, Yoshihisa Harada, Yuki Orikasa, and Yoshiharu Uchimoto	Chemistry of Materials	36	4	1928-1940	2024
7	Double-Layered Perovskite Oxyfluoride Cathodes with High Capacity Involving O–O Bond Formation for Fluoride-Ion Batteries	Hidenori Miki, Kentaro Yamamoto, Hiroyuki Nakaki, Takahiro Yoshinari, Koji Nakanishi, Shinji Nakanishi, Hideki Iba, Jun Miyawaki, Yoshihisa Harada, Akihide Kuwabara, Yanchang Wang, Toshiki Watanabe, Toshiyuki Matsunaga, Kazuhiko Maeda, Hiroshi Kageyama, and Yoshiharu Uchimoto	Journal of the American Chemical Society	146	6	3844-3853	2024
8	Hydrogen-Bonded Structures of Water Molecules in Hydroxy-Functionalized Nanochannels of Columnar Liquid Crystalline Nanostructured Membranes Studied by Soft X-ray Emission Spectroscopy	Kazuma Hamaguchi, Takeshi Sakamoto, Naoya Kurahashi, Yoshihisa Harada, and Takashi Kato	The Journal of Physical Chemistry Letters	15	2	454-460	2024
9	Determining factor of orbital torque efficiency in ferromagnet/Cu/Oxide thin films	Junyeon Kim, Jun Uzuhashi, Masafumi Horio, Tomoaki Senoo, Toshihide Sumi, Dongwook Go, Daegeun Jo, Iwao Matsuda, Tadakatsu Ohkubo, Seiji Mitani, Hyun-Woo Lee, and YoshiChika Otani	Phys. Rev. Materials	7		L111401	2023
10	Oxide layer dependent orbital torque efficiency in ferromagnet/Cu/oxide heterostructures	Junyeon Kim ,Jun Uzuhashi,Masafumi Horio, Tomoaki Senoo, Dongwook Go,Tetsuya Wada, Iwao Matsuda,Tadakatsu Ohkubo, Seiji Mitani, Daegeun Jo,6 Toshihide Sumi, Hyun-Woo Lee, and YoshiChika Otani	Physical Review Materials	7	11	L111401	2023
11	Structure and Electronic State of Boron Atomic Chains on a Noble Metal (111) Surface	Y. Tsujikawa, X. Zhang, M. Horio, F. Komori, T. Nakashima, Y. Ando, T. Kondo, I. Matsuda	e-Journal of Surface Science and Nanotechnology	22	1	1-8	2023
12	Hydrogen-induced sulfur vacancies on the MoS2 basal plane studied by AP-XPS and DFT calculations	Fumihiko Ozaki, Shunsuke Tanaka, YoungHyun Choi, Wataru Osada, Kozo Mukai, Mitsuaki Kawamura, Masahiro Fukuda, Masafumi Horio, Takanori Koitaya, Susumu Yamamoto, Iwao Matsuda, Taisuke Ozaki, Jun Yoshinobu	ChemPhysChem	24		e202300477	2023
13	Resonant photoemission spectroscopy of atomic layer Fe 2 N on Cu(111) with continuous angular rotation of linearly polarized light	M. Horio, Y. Kudo, T. Wada, T. Sumi, Y. Hirata, M. Niibe, F. Komori, and I. Matsuda	J. Phys.: Condens. Matter	35	42	425001	2023

E-labo. Spin Paper 2023

No.	Title	Authors	Journal	Vol.	No.	Page	Year
1	Time-, spin-, and angle-resolved photoemission spectroscopy with a 1-MHz 10.7-eV pulse laser	Kaishu Kawaguchi, Kenta Kuroda, Z. Zhao, S. Tani, A. Harasawa, Y. Fukushima, H. Tanaka, R. Noguchi, T. Iimori, K. Yaji, M. Fujisawa, S. Shin, F. Komori, Y. Kobayashi, and Takeshi Kondo	Review of Scientific Instruments	94		083902	2023
2	Topological surface state of Bi_2Se_3 modified by physisorption of n-Alkane	Rena Moue, Hiroto Yamazaki, Tatsuya Kitazawa, Koichiro Yaji, Hiroshi Yaguchi, Kenta Kuroda, Takeshi Kondo, Ayumi Harasawa, Takashi Iwahashi, Yukio Ouchi, Shik Shin and Kaname Kanai	ChemNanoMat	9		e202200538	2023